Available online at www.sciencedirect.com

SciVerse ScienceDirect

Energy Procedia 24 (2012) 212 – 228

Energy Procedia

DeepWind, 19-20 January 2012, Trondheim, Norway

GPS synchronization and EMC of harmonic and transient measurement equipment in offshore wind farms

Łukasz Hubert Kocewiak[a]*, Iván Arana[a], Jesper Hjerrild[a], Troels Sørensen[a], Claus Leth Bak[b], Joachim Holbøll[c]

[a]DONG Energy A/S, Kraftværksvej 53,7000 Fredericia, Denmark
[b]Institute of Energy Technology, Aalborg University, Pontoppidanstræde 101, 9220 Aalborg, Denmark
[c]Technical University of Denmark, Elektrovej 329, 2800 Lyndby, Denmark

Abstract

The challenges of harmonic and transient measurements in wind farms are described in this paper. It is shown that appropriate measurements of harmonic and transient phenomena in offshore wind farms are essential for data analysis and model creation/validation of components or subsystems. The GPS synchronization, electromagnetic compatibility (EMC) and interference (EMI) challenges during the development, construction, testing and installation of a measurement system for multi-point, high-speed and long-term data logging is described in this paper. The presented measurement system was tested in a rough offshore environment at Avedøre Holme and Gunfleet Sands offshore wind farms.

The paper will describe the application of GPS technology in synchronised measurements carried out at Avedøre Holme and Gunfleet Sands wind farms. Different aspects of software development and hardware configuration in order to optimise measurement system´s reliability during offshore measurements will be presented. Also real-life examples of results from both offshore measurement campaigns will be described. Some limitations, improvements and results of the measurement system will be explained from both harmonic and transient measurements. The paper clearly presents possible electromagnetic interference in wind turbines that can affect measurements. Also the application of appropriate mitigation techniques such as data acquisition board configuration, coaxial cable leading, as well as usage of EMC-proof boxes for high frequency measurements is described.

Keywords: GPS synchronization; EMC; EMI; harmonic measurements; offshore wind farm; transient measurements.

* Corresponding author. Tel.: +45 99557851.
E-mail address: lukko@dongenergy.dk.

 doi:10.1016/j.egypro.2012.06.103

1. Introduction

Accurate measurements of harmonic and transient phenomena in offshore wind farms (OWFs) are essential for data analysis and model creation/validation of components or subsystems. Afterwards, these models can be used in simulation tools during the development of offshore wind farms. Due to the importance of measurements it was decided to perform long term measurement of harmonic emission and high-speed measurements of switching transients in OWFs [1]. In order to observe the harmonic and transients in the collection grid without any misleading disturbances, a great deal of effort was taken to make the measurements as accurate as possible.

The measurement system developed here was designed taking into account the special application, requirements and environment of OWFs. Here, the access is limited due to weather conditions and significant operational costs; hence a robust and trustful measurement system is important. The synchronization of measurements, electromagnetic compatibility (EMC) and electromagnetic interference (EMI) are important aspect taken into consideration during the design of the measurement system. The synchronization of measurement systems in different locations is a critical aspect taken into account in the development process of a flexible measurements system for harmonic and transient measurements in OWFs.

The recorded measurements in Avedøre Holme (AVV) and Gunfleet Sands (GFS) will be used for two ongoing PhD's as well as future R&D projects at DONG Energy.

2. EMC in offshore wind farms

In general, EMI could occur during harmonic and transient measurements, if there is a transfer of electromagnetic energy from a source, through a coupling path to a receptor. The EMI source in a wind turbine (WT) and transformer platform could be the main 33 kV power circuit and the EMI receptor could be the measurement equipment.

For the harmonic measurements in a WT, the power converter is the most likely source of EMI. On the other hand, for the transient measurements, the switching operations of a vacuum circuit breaker (VCB) generate fast transient overvoltages that could induce voltage in the measurement equipment. These two possible sources of EMI had to be considered for the development of the measurement system.

2.1. EMI during harmonic measurements

The most likely scenario for incompatibility occurs when a relatively high power circuit (i.e. power converter) is located near a very sensitive receptor (e.g. sensors, cables, measuring head unit) [2], [3]. This is a reality in the switch-mode high power density converters commonly used in modern wind turbines; that are potential generators of EMI due to the switching action of the converter

The switching action generates a spectrum of the switching frequency and its harmonics. The main noise sources of switching frequency harmonics are the switched currents and the commutating diode. This noise is a combination of the switching frequency and its associated rise time (approximately 100 ns) and turn on spikes caused by the diode recovery current. This recovery current spike occurs at the end of a diode conduction cycle when reverse voltage is just applied by the transistor [2].

2.2. EMI during transient measurements

During the switching operations of a gas insulated switchgear (GIS), fast transient overvoltages are generated. These transient overvoltages produce multiple transient fields, which could induce currents on the metallic sheet of measuring cables [4]. These transient currents, could develop voltages on the central conductor of the measuring cable via transfer impedance and by a mechanism of the pigtail coupling [5].

Recent work has been done on calculation of transients induced on control cables in GIS [6], and air isolated substations at 69 kV [7]. However, no work has been done regarding MV VCB with metal

enclosure, where the switching device and busbars are contained in a stainless steel tank filled with SF6. These are typical switchgear cubicles used in OWFs due to its breaking current ratings, compactness and maintainability.

The reason behind the lack of research in this area is that due to the several metal enclosures, no EMI is expected outside of the switchgear cubicle. Hence, no interference was expected during the transient measurements, since the switchgear cubicle and the EMC box where the measurement equipment was installed, remained closed during the measurements.

3. Avedøre Holme and Gunfleet Sands Wind Farms

AVV and GFS OWFs are two OWFs partly owned by DONG Energy where the measurements system was installed. The WTs used on both OWFs are Siemens Wind Turbine SWT-3.6. Once the measurement system was proven to be reliable under offshore conditions for short term and long term measurements in AVV, the system was installed in GFS.

In the WTs in AVV and GFS, the LV voltage and current probes were installed in the auxiliary switchboard; while the MV voltage and current probes were installed in the transformer side of the VCB. The measuring locations within the collection grid of GFS were the transformer platform, the first turbine of a radial and the last turbine of a radial. The MV voltage and current in the transformer platform were installed in the cable side of the VCB of the radial. The LV and MV voltage and current measurements within the WTs in GFS, were the same as the ones in AVV.

3.1. Wind farms description

AVV OWF in the south of Copenhagen is a shared project between DONG Energy and Hvidovre Vindmøllelaug A/S. A location so close to shore and easy accessibility to the offshore WTs via a footbridge is the basic idea behind the project. This gives DONG Energy a unique opportunity to test and try out new WT concepts, before they are implemented in large scale OWFs.

GFS OWF is located on the east cost of the UK and consists of two phases, one with 30 WTs and another with 18 turbines. The WTs are connected in “rows” by 36 kV submarine cables. Each pair of rows is then connected by one “root” cable and later in the substation to a MV busbar via a VCB. Two park transformers (120 MVA, 132/33 kV) are placed in the center of the wind farm in the offshore substation. From the substation the electricity is transmitted to shore via a 8.5 km long submarine cable which connects to the Clacton substation at Cooks Green (see Fig. 1).

3.2. Wind turbine description

The SWT-3.6-107 and SWT-3.6-120 are variable-speed WTs utilizing full scale frequency converters. The frequency converter system comprises two AC/DC converters and a DC-link decoupling the variable-frequency generator and the grid frequency. There is a transformer to step-up the voltage on each of WTs. The WT transformer is connected with a VCB to the MV network.

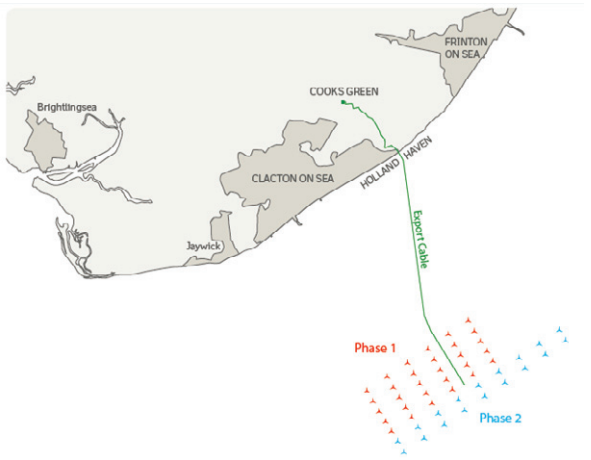

Fig. 1 Gunfleet Sands Offshore Wind Farm located on the east cost of the UK close to Clacton on Sea.

4. Methods

All measurement set-ups face some level of error due to systematic (bias) and random (noise) error sources. By appropriate design of the system, sensor selection, sensor installation, sensor calibration, data acquisition (DAQ) calibration and an accurate synchronization board; the systematic and random error can be significantly reduced. Moreover, in order to reduce electromagnetic interference (EMI) from the power system to the measurement system, a custom made EMC box was designed as well as sophisticated shielding solutions.

4.1. Synchronization board

Specially designed EMC-proof boxes were equipped with cooling system in order to keep constant ambient temperature. If the ambient temperature differs from the calibration temperature by more than ±5°C the temperature compensated crystal oscillator (TCXO) will be affected by drift and introduce additional synchronization uncertainties.

4.2. Software development

In software development it is of special importance to implement synchronization support in the easiest way as possible. In case of transient measurements synchronization delays affected by the software layer can affect the whole measurement process. It was decided that the measurement software will start according to the time reference obtained from timing and synchronization board. A time reference is an external source of timestamp that provides periodic time updates. It is possible to provide time reference from GPS satellites, IEEE 1588 masters, or IRIG-B sources. As mentioned earlier each of the sources provides periodic time updates. In case of GPS satellites broadcast the current time once per second, on the second's boundary. The synchronization board has the oscillator (clock) accuracy of 1 ppm which provides accurate time reference every second (PPS).

In order to configure the driver on the software layer in the simplest and most efficient way a linear structure was used. It was done in the following way:

- Initialize driver: initializes a session to the timing and synchronization board, which is the first required step before any I/O operation (e.g. digital triggering on the hardware level) can be performed.
- Enable trigger: the timing and synchronization board is ready to start time stamping on the specified input terminal (i.e. triggering on the hardware level). Any trigger that occurs on the specified input terminal with the specified active edge is time stamped.

- Read trigger timestamp: the oldest, non-read time stamp associated with the specified terminal is returned.
- Disable timestamp trigger: disables time stamping on the specified terminal.
- Close driver: stops all ongoing operations associated with the session and all the resources can be used later is needed.

4.3. Synchronization uncertainties

Used for offshore measurement purposes receivers provide a 1 pps on-time pulse. The GPS receiver is limited to using SPS the uncertainty is defined by the top row in Table 1. It shows that there is a 50 % probability that a given on-time pulse from GPS will be within ±115 ns of UTC. The 1σ uncertainty of GPS (~68 % probability) is ±170 ns, and the 2σ uncertainty (95 %) is ±340 ns [8], [9].

Table 1 Timing uncertainty of GPS in One-Way Mode.

Service	Uncertainty (ns) 50th percentile	Uncertainty (ns) 1σ	Uncertainty (ns) 2σ
SPS	±115	±170	±340
PPS	±68	±100	±200

To achieve uncertainties presented in Table 1 one has to calibrate receiver and antenna delays, and estimate synchronization errors. The antenna providing reliable performance in harsh radio frequency (RF) jamming environments was connected to the receiver and mounted outdoors where it had clear, unobstructed view of the sky. This condition can be easily satisfied in large OWFs situated far from natural barriers and effects such as multipath propagation [10] due to the signal reflection, and high dilution of precision (DOP) when detected satellites are close together in the sky, can be neglected. Positional accuracy was improved due to the fact that the WTs and the substation at GFS OWF are situated far from each other and naturally are far from multipath reflectors (see [11]).

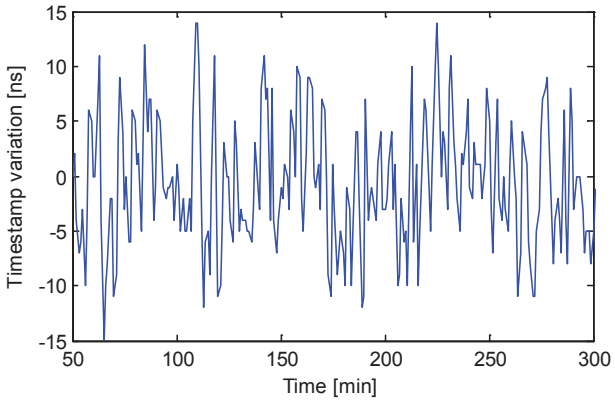

Fig. 2 Variation of pulse-per-second signal synchronized with a GPS timestamp using phase-locked loop.

It is important to mention that in all location data were acquired using the same DAQs with the same sampling rate, so phenomena such as filter delay does not affect the synchronization effectiveness. Also RG59/U coaxial cables with the same length of 30 m were used to connect the active GPS antenna with the timing and synchronization board, which means the propagation delays were the same.

Pulse-per-second signal accuracy measured during measurement campaign at Gunfleet Sands OWF is shown in Fig. 2. The accuracy is even better than provided by the manufacturer (15 ns, 1σ).

4.4. Installation considerations

The measurement equipment in the wind turbines in Avedøre and Gunfleet Sands was installed in the basement of the wind turbine, where the service technicians do not require going often. In the transformer platform the measurement equipment was installed in the 33 kV switchgear room, close to the voltage and current probes.

It is important to mention, that the installation of the GPS antennas in Avedøre and Gunfleet Sands had to be done in open space outside the wind turbines and the transformer platform, in order to receive the best signal from the satellites. Nevertheless, the measurement equipment should be installed indoor, in a controlled environment. These two opposite requirements for the entire measurement system had to be fulfilled.

This was solved in the wind turbines in Avedøre and Gunfleet Sands, by installing the GPS antennas outside the turbine tower in the service stairs to enter the wind turbine, with the coaxial cable though a service opening in the turbine tower. This is shown in Fig. 3. The GPS antenna in the transformer platform was installed in the platform upper level, close to the helipad, to reduce the possibility of interference with high structures. Then, the coaxial cable was lowered though the transformer hall, until the flexible cable sealing system that connects the transformer hall with the 33 kV switchgear room. This is shown in Fig. 4.

Fig. 3 GPS antenna installed on the service stairs of a wind turbine in Gunfleet Sands.

Fig. 4 GPS antenna installed on the platform upper level in Gunfleet Sands.

4.5. Measurement system design

For such specific measurement purposes like harmonic and transient measurements, National Instruments (NI) instrumentation was used. The test equipment consists three PXI-1033 chassis which each of them comprises PXI-6682 timing and synchronization board with Trimble Bullet III GPS antenna used to read GPS timestamp, PXI-4472 dynamic signal acquisition (DSA) board with second-order low-pass anti-aliasing filter [8] applied in case of harmonic measurements and PXI-6133 multifunctional board used for transient measurements. The chassis is connected to a portable computer via ExpressCard

laptop host. Used MXI-Express remote controller achieves up to 110 MB/s sustained throughput. The measurement PC units used for measurements comprise Intel Core 2 Duo T9400 @ 2.53 GHz CPU, 4 GB @ 800 MHz RAM, Windows Vista Enterprise operating system (OS) and Seagate ST95005620AS Hybrid-HDD.

The frequency band of interest in case of the harmonic measurements is much lower, than for transient measurements, so the same probes were used in both cases. Such demanding frequency range of interest during the transient measurements, creates additional problems with EMI. However, for the selection of the DSA card for transient measurements, no high frequency components were expected; therefore no additional anti-aliasing filtering was provided

4.6. Sensors

Precisely selected sensors were used for transient measurement purposes. It was expected to carry out measurements with sample rate up to of 2.5 MS/s/ch which requires sensors with a flat bandwidth (±3 dB) at least up to 1.25 MHz. Different sensors were used to measure in the LV and MV in AVV and GFS. At 0.69 kV in the WTs differential voltage sensors were used, while for the 10 kV and 33 kV in AVV and GFS a custom made probe was used. The AC current Rogowki coils in the LV and MV used in AVV and GFS were the same.

4.6.1. Voltage probes

SI-9001 differential voltage sensors with bandwidth of DC-25 MHz were used in the LV in the WTS. In the MV, capacitive voltage sensors installed as “dead-end” T-connectors with bandwidth of 1Hz-1 MHz were installed. These MV T-connector were installed to the MV network as a “dead-end” and the phase-to-earth voltage is measured using an end-plug. Since the capacitive end-plug is not normally used for precision measurements, an amplifier for precision measurements with high frequency response developed by DELTA has been used [12].

4.6.2. Current probes

In order to measure currents Powertek CWT3LF and CWT30LF flexible Rogowki coils were used with 0.055Hz-3MHz minimum bandwidth. The cable from sensor to integrator is a fixed-length double screened RG58 type which is suitable to be used in harsh WT electromagnetic environment, as well as in the transformer platform. The cable is relatively long (8m) and cable parasitic capacitance is compensated to achieve flat performance within the bandwidth. Also the integrator by its low-pass filter nature is suitable to attenuate EMI.

4.7. Sensor installation

In the wind turbine of AVV the LV voltage probes were installed in the auxiliary switchboard, DC/AC converter and DC-link of the wind turbine. The LV current probes were installed on the output terminals of the DC/AC convert, DC-link and LV side of the WT transformer. The MV voltage and current probes in the WTs were installed in the WT transformer side of the VCB.

The measuring locations within the collection grid of GFS were the transformer platform, the first turbine of a radial and the last turbine of the same radial. Within the WTs, the LV voltage and current probes were installed in the auxiliary switchboard. The MV voltage and current probes in the WTs were installed in the transformer side of the VCB; while in the substation the voltage and current probes were installed in the cable side of the VCB of the radial.

In AVV and GFS, the measurement equipment was install by professional electricians, and tested after the installation was complete. In general all the sensitive measurement equipment was installed inside the EMC box when possible.

4.8. DAQ

Different type of noise can affect the overall measurement process. The first type, known as differential mode (DM) noise, is propagated out one wire and other wire carries noise exactly equal and opposite. DM noise amplitudes are usually minimal above 2 MHz because line-to-line or line-to-ground capacitance and wiring inductance tend to filter this type noise [2]. The other type of conducted noise, common mode (CM) noise, travels in the same direction in both wires and returns through the ground. CM noise, requires a different type filter. CM filters are usually CM chokes. Such choke relies on the magnetic properties of ferrite cores to absorb CM noise and were used during measurements as presented in [13].

During measurements carried out in the WFs dynamic signal acquisition (DSA) cards with two-pole low-pass Butterworth filter were used. Taking into consideration Nth-order Butterworth filter one can describe it in terms of energy spectra (squared magnitude) which has form

$$|H(\omega)|^2=\frac{1}{1+(\omega/\omega_c)^{2N}} \qquad (1)$$

where ω_c is -3 dB cut-off frequency. The Butterworth approximation of ideal low-pass filter has only poles (i.e. no finite zeros) and yields a maximally flat response around zero and infinity. This approximation is also called maximum flat magnitude (MFM). This feature becomes extremely important in case of harmonic measurements where each frequency within passband has to be filtered in the same way [14].

4.9. Noise consideration

Different type of noise can affect the overall measurement process. The first type, known as differential mode noise, is propagated out one wire and other wire carries noise exactly equal and opposite. Differential mode noise amplitudes are usually minimal above 2MHz because line-to-line or line-to-ground capacitance and wiring inductance tend to filter this type noise [2]. The other type of conducted noise, common mode noise, travels in the same direction in both wires and returns through the ground. Common mode noise, requires a different type filter. Common mode filters are usually common mode chokes. Such choke relies on the magnetic properties of ferrite cores to absorb common mode noise and were used during measurements as presented in Fig. 5 [13].

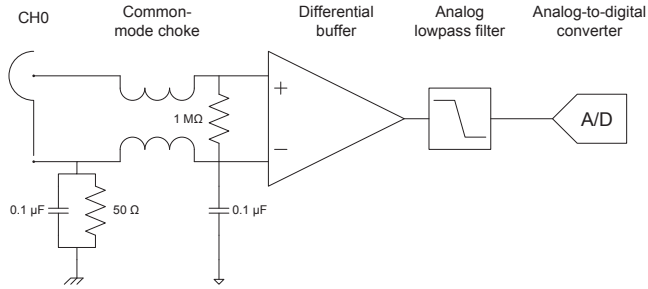

Fig. 5 National Instruments 4472 data acquisition board analog block diagram.

4.10. Cross-talk

Crosstalk is observed when in a data acquisition device signal transmitted on one channel creates unwanted effects in another adjacent channel. Crosstalk is mostly affected by undesired coupling between neighboring channels. In theory each of analog inputs in measurement system should exhibit normally distributed noise during open circuit measurements. In case of crosstalk additional harmonic component can be observed in measurements.

In wind turbine measurements the fundamental component should be the most significant harmonic seen due to crosstalk in adjacent channels. Normally manufacturers of data acquisition devices should provide in specification parameters associated with this phenomenon.

4.11. GPS synchronization

As mentioned before, a PXI-6682 timing and synchronization board with Trimble Bullet III GPS antenna was used in each measurement location to read GPS timestamp. During the offshore measurement, the receivers provide a 1 pps on-time pulse. The GPS receiver is limited to using SPS, which has 50 % probability that a given on-time pulse from GPS will be within ±115 ns of UTC. The 1σ uncertainty of GPS is ±170 ns, and the 2σ uncertainty is ±340 ns [8].

4.12. EMC box

The EMC box used for in the three measurement locations are standard EMC enclosure type AE from Rittal A/S with the dimensions 380x600x350 mm (WxHxD). At 1 MHz the electrical field attenuation for this enclosure type is 100dB and 45dB of magnetic attenuation.

The EMC boxes are made from steel sheets with aluminum zinc coating, and powdered coated in RAL 7032 on the outside. Additionally, an EMC filter-fan system was installed in the boxes to maintain a constant temperature inside the box, since they remained closed during the measurements. The EMC filter-fan system provided a constant ambient temperature by continuous forced air cooling because if the ambient temperature surrounding the DAQ board differs from the calibration temperature by more than ±5°C the results can be disturbed and it is recommended to recalibrate the DAQ board.

To supply all the measurement equipment a 25 A filter was mounted in the EMC box. All the measurement equipment was grounded to the central earthing point inside the EMC box, and this was further grounded in each measurement location.

It was decided to make a 10 cm hole on one side of the EMC box to be able to connect different equipment outside the EMC box. Finally, it was calculated that the EMI from the measurement system to the power system could be ignored, since the DAQ input impedance is 1 MΩ; therefore energy drawn from sensors (loading error) could be neglected.

Fig. 6 shows the EMC box installed in the transformer platform. The NI chassis, EMC fan, EMC filter, power supply, current probes and UPS can be seen.

Fig. 6 EMC box installed in the transformer platform at Gunfleet Sands Offshore Wind Farm.

4.13. Measurement uncertainties

Precision and accuracy are terms used to describe systems and methods that estimate, measure, or predict. The method provides a measured value, which is wanted to be as close to the true value as possible. Precision and accuracy are ways of describing the error that can exist between these two values [15], [16].

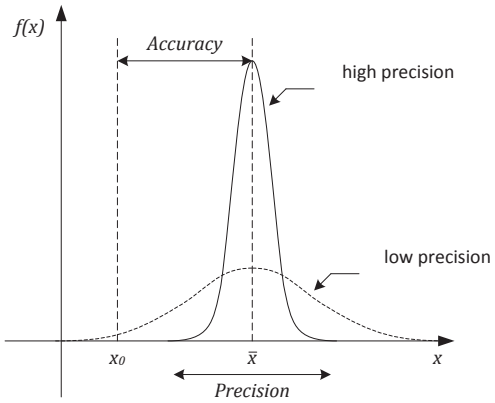

Fig. 7 Accuracy indicates proximity of measurement results to the true value, precision to the repeatability or reproducibility of the measurement.

Poor precision results from random errors while poor accuracy results from systematic errors and is usually dependent on how the measurement equipment is calibrated (see Fig. 7). While random errors occur instantaneously, in the course of the measurements, the actual values of systematic errors are predetermined before the measurements get started. Therefore it is of great importance to be certain about possible systematic errors before measurement process is started in order to compensate errors and improve the accuracy. Random errors have to be attributed to small fluctuations of estimated values which affect the measuring process and prove to be uncontrollable. According to experience, the random errors of stationary experimental set-ups may be considered, at least in reasonable approximation, to follow a normal probability distribution. Due to fact that it is not a straight forward task to understand these phenomena in detail, some guidance in the central limit theorem of statistics [17] can be found. According to this, loosely stated, the superposition of sufficiently many similar random perturbations tends to a normal distribution [18].

A random variable is said to be normally distributed with parameters μ and σ^2, and can be written $X \sim N(\mu,\sigma^2)$, if its probability density function is [19], [20]

$$f(x)=\frac{1}{\sqrt{2\pi}\sigma} e^{-(x-\mu)^2/2\sigma^2},\ -\infty<x<\infty \qquad (2)$$

Precision of the measurement, and is expressed by quoting standard deviation, or signal-to-noise ratio. If a measurement with true random error is repeated a large number of times, it will exhibit a Gaussian distribution. More precisely saying if X_1, X_2, …, X_n is a sequence of independent and identically distributed (IID) random variables with mean μ and finite positive variance σ^2. If $S_n=X_1+\ldots+X_n$, then

$$Z_n=\frac{S_n-n\mu}{\sigma\sqrt{n}} \qquad (3)$$

The central limit theorem (CLT) states that as the sample size n increases, the distribution of the sample average of X_i approaches the normal distribution irrespective of the shape of the common

distribution of the individual terms X_i. Random variables will converge in distribution to the standard normal distribution N(0,1) as n approaches infinity. N(0,1) is thus the asymptotic distribution of Z_n [21]

The precision of the measurement is normally quantified by the standard deviation σ that indicates the width of the Gaussian distribution. Given a large number of measurements, a total of 68 % of the measurements will fall within ±1σ of the mean, 95 % will fall within ±2σ; and 99.7 % will fall within ±3σ. The smaller the standard deviation is, the more precise the measurements are.

4.14. Noise consideration

Signal-to-noise ratio [22] is defined as the power ratio between a signal and the background noise

$$SNR_{dB}=10\log_{10}\left(\frac{P_{signal}}{P_{noise}}\right)=10\log_{10}\left(\frac{A_{signal}}{A_{noise}}\right)^{2}=20\log_{10}\left(\frac{A_{signal}}{A_{noise}}\right) \quad (4)$$

Before signal as meaningful information is logged it is also recommended to measure input noise level on order to assess the measurement precision [23].

5. Results

If during measurements the transfer of electromagnetic energy from source (emitter) equipment, which in a WT is the main power circuit, through a coupling path to a receptor (receiver), which is the measurement equipment, an EMI occurs.

5.1. Cross-talk measurements

Before any measurements are carried out it is recommended to perform test of EMI in the environment. Also in case of offshore measurements such test measurement s were done. The first step is to perform open circuit measurements in the field and compare with laboratory expectations. According to central limit theorem one should expect normally distributed noise in open circuit measurements. As it can be seen from Fig. 8 and Fig. 9 open circuit measurements performed in the laboratory are normally distributed.

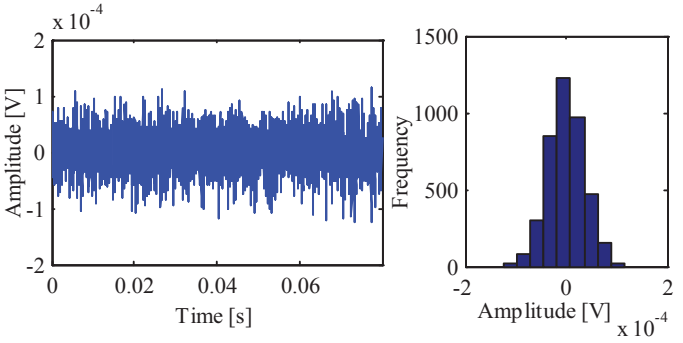

Fig. 8 Open circuit measurement carried out in the lab and normally distributed histogram.

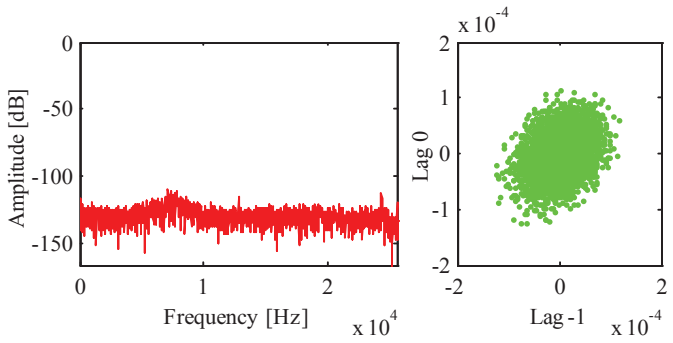

Fig. 9 Open circuit measurements estimated spectrum and lag plot.

Please note that the crosstalk for adjacent channels is lower than -80dB in used for harmonic measurement dynamic signal acquisition board from National Instruments, i.e. Pxi-4472. Taking into consideration cross-talk from adjacent channels additional harmonic components can be seen at the top of Gaussian noise. Cross-talk measurements can be seen in Fig. 10 and Fig. 11.

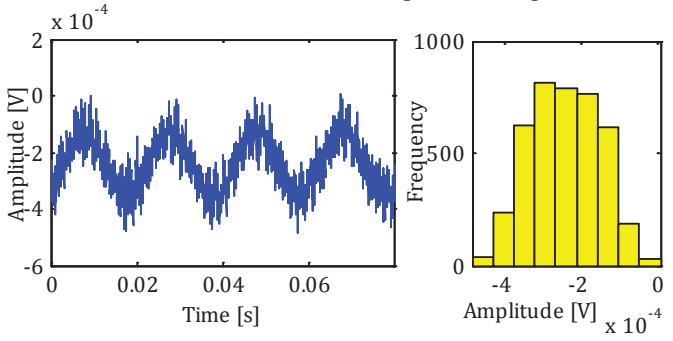

Fig. 10 Open circuit measurements with cross-talk carried out in the lab.

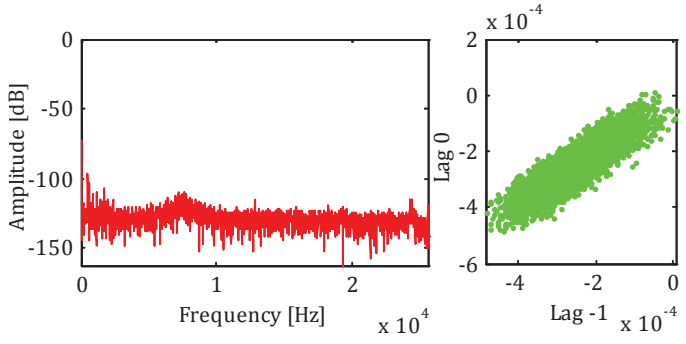

Fig. 11 Open circuit measurements with cross-talk estimated spectrum and lag plot.

5.2. Converter interference

The most likely scenario for incompatibility occurs when a relatively high power circuit (i.e. power converter) is located near a very sensitive receptor (e.g. sensors, cables, measuring head unit) [2], [3]. Switch-mode high power density converters commonly used in nowadays wind turbines are potential generators of EMI due to the switching action of the converter The switching action generates a spectrum of the switching frequency and its harmonics. The main noise sources of switching frequency harmonics

are the switched currents and the commutating diode. This noise is a combination of the switching frequency and its associated rise time (approximately 100 ns) and turn on spikes caused by the diode recovery current. This recovery current spike occurs at the end of a diode conduction cycle when reverse voltage is just applied by the transistor [2].

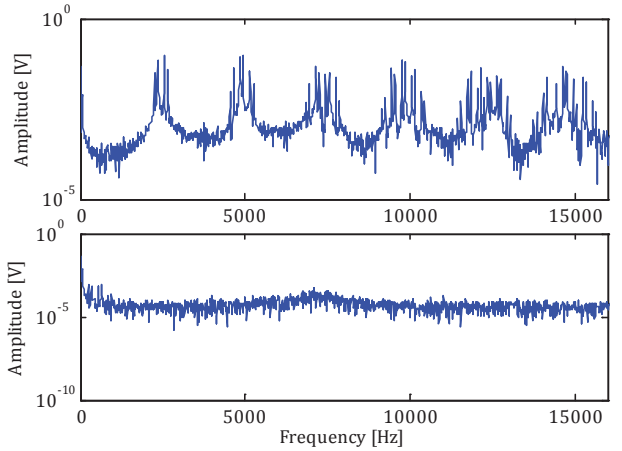

Fig. 12 Estimated spectrum of open circuit channel during wind turbine production (top) and during not switching operation (bottom).

Fig. 12 presents estimated spectrum of measured open circuit channel. When the grid-side converter is operating (i.e. wind turbine is producing) it is possible to see spectrum affected by the converter modulator. It is worth to emphasize that the interference is much more significant than the noise level. When the wind turbine is not producing and the grid-side converter is shut-down only crosstalk phenomenon as presented in Fig. 10 can be observed.

In both Fig. 12 as well as Fig. 13 the fundamental component interference can be easily observed. It is due to the fact that in the neighboring analog input voltage channel the voltage at the converter AC terminals is measured. In that case the fundamental component is available in case of wind turbine production and in case of its switch off. When the wind turbine is shutdown the grid voltage is measured which comprises the grid fundamental frequency as well as few significant baseband harmonic components. Such phenomenon can be easily seen from multi-resolution time-frequency analysis presented in Fig. 13.

Time-frequency representation of measured continuous-time signals achieved using continuous wavelet transform is presented in Fig. 13. In order to analyze measured signal which statistics vary in time and exhibits some oscillations non-orthogonal complex Morlet mother wavelet base was used. The figure shows how different frequency components affects measured open circuit channel from the 4472 data acquisition board working inside the wind turbine. It can be seen that within the first period (0-0.14 s) the wind turbine is producing and frequency components around 2.5 kHz and 5 kHz generated by the modulator of the grid-side converter can be easily observed. Later the WT is stopped and only harmonics affected by the external network can be measured.

The channel was measured by SI-9001 voltage differential probe which full scale (FS) range is ±7 V and input voltage differential range is ±700 V. As it can be seen from Fig. 13 (top) the measured noise is less than 1 % of FS and does not affect measurements significantly. Still it has to be emphasized that the interference is much higher when the power electronic equipment of the main power circuit in the WT is in operation. Normally open circuit measurements performed in laboratory conditions are very close to Gaussian distribution. Additionally it has to be emphasized that the crosstalk for adjacent channels is lower than -80 dB and the idle channel noise for applied sample rate (44.1 kS/s) is -94 dBVmax.

The width of a wavelet function is defined here as the e-folding time of the wavelet amplitude and for Morlet wavelet basis function is equal to $\sqrt{2}s$, where s is a wavelet scale. The black line in Fig. 13

indicates cone of influence (COI), region of the wavelet spectrum in which edge effects became important as the e-folding time for each at each scale [24].

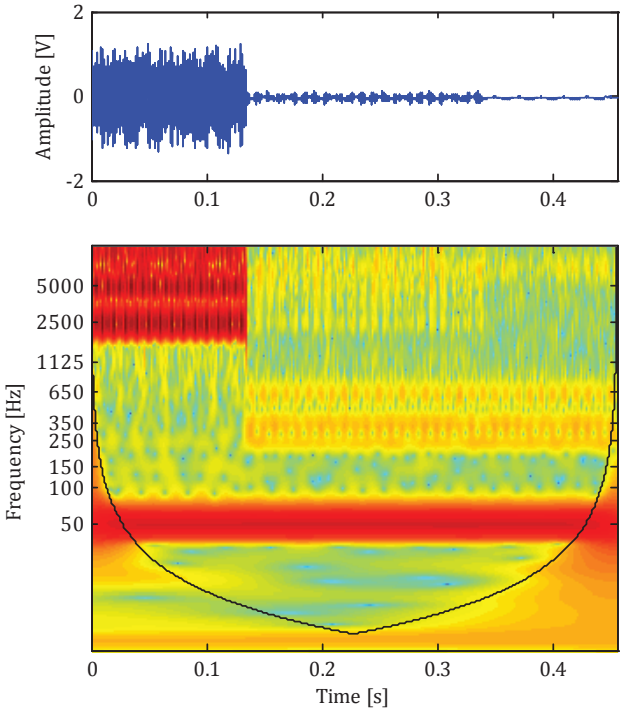

Fig. 13 Continuous wavelet transform showing electromagnetic interference in the wind turbine.

From measurements it can be seen that signal-to-noise ratio which is defined by Eq. 4 is significant for higher frequencies. Some estimated signal-to-noise ratios around certain frequencies (i.e. carrier groups) in wind turbine measurements are presented in Table 2.

Table 2 Estimated signal-to-noise ratios around carrier groups in measured output voltage of the grid-side converter

Carrier group	Frequency [Hz]	Value [dB]
1	2500	55
2	5000	48
3	7500	48
4	1000	39
5	12500	32

This shows that the analysis of frequency components above 2 kHz can provide inaccurate results. This also indicates that sample rate above 4 kS/s/ch is not necessary for long-term harmonic measurements. Please note that in practice the noise level in the estimated spectrum is also strongly dependent on the window length of analyzed signal.

5.3. Transient measurements synchronization in AVV

Some of the transient measurements during the switching in of the VCB in the AVV wind turbine are shown in Fig. 14. In this figure the voltage and current on the MV side of the transformer are shown, as well as the LV side voltage. It is possible to see in this figure the high frequency voltage oscillation caused by the pre-strike in the VCB that is transfer to the LV side as well as the inrush current of the transformer.

The VCB model validation, as well as the wind turbine transformer and external grid validation has been reported in [25].

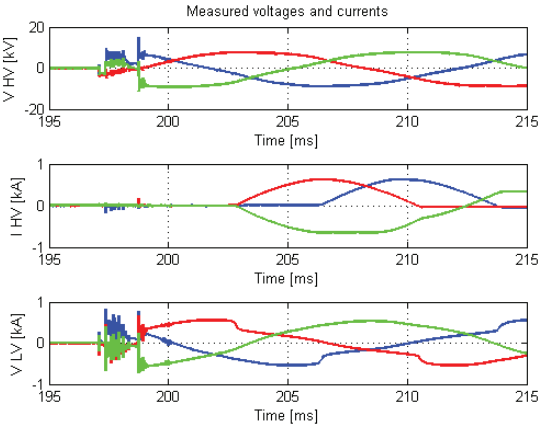

Fig. 14 Measured three-phase voltages and currents, during the closing operation of the MV VCB in the wind turbine of AVV from 195 to 215 ms. The voltage on the primary side of the transformer is shown in the top, the current on the primary side of the transformer.

5.4. Transient measurements synchronization in GFS

Due to maintenance, in large offshore wind farms the MV VCB in the offshore substation could be operated several times a year. These normal switching operations would cause transient overvoltages in the collection grid that will move along the energized radials. Such transient overvoltages were measured in GFS during the measurement campaign.

The measured voltages in the offshore substation (OS) and the last turbine in a radial (F9), during the energization of a cable connected parallel to the measured radial is shown in Fig. 15. Here it is possible to see how a voltage dip and a small voltage transient are measured in the three phases and both locations. The voltage dip is caused after the cable connection (left subplot); while the small voltage transient on top of the voltage dip (right subplot) is caused by the VCB operation in the offshore wind farm substation. This small voltage transient appears first in the offshore substation at 60 ms, and then travels for 22 μs to the last turbine in the radial (F9) and finally back to the offshore substation. The 22 μs corresponds to the travelling time the voltage wave would take to travel from the offshore substation to wind turbine F9 based on the different cables' parameters and lengths.

The measured travelling speed of the voltage wave, corresponds half the speed of light, reported previously by similar switching operations recorded in Nysted offshore wind farms [12].

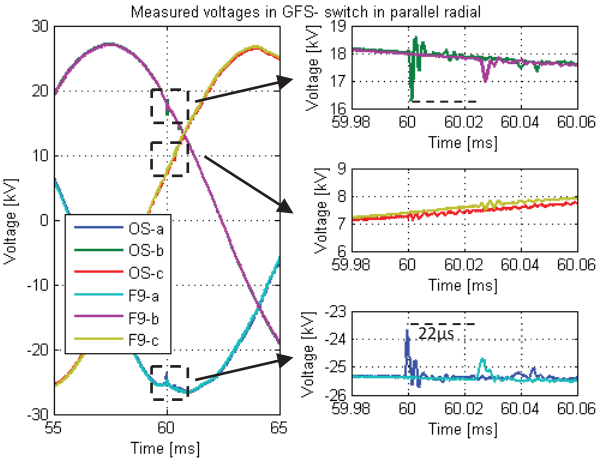

Fig. 15 Measured three-phase voltages, during the energization of a parallel cable in GFS from 55 to 65ms. The three-phase voltages on the offshore substation (OS) and the last wind turbine in the radial (F9) are shown in the left subplot, while a zoom in on each individual phase is shown in the three right subplots

6. Discussion

During the removal of the measurement equipment in GFS, after 8 months of measurements, it was noticed that one of the GPS antennas was damaged. The antenna presented high level of corrosion in the metallic lower part of the antenna. Only the antenna in one of the wind turbines presented this corrosion. Due to this deterioration, the coaxial cable connected to the antenna, was also damaged, and had to be repaired afterwards. The metallic part of the antenna was simply cleaned. The damage in the antenna clearly shows the harsh environment to which the offshore wind turbines are subjected. In practice, this is solved by carefully isolating the equipment inside the turbine tower from the offshore environment.

Electromagnetic interference during measurements in offshore wind farms is an important issue and requires special considerations. It was shown that grid-side converters in wind turbines can be significant sources of possible interference during measurements. In case of harmonic measurements, where frequency components of amplitude around 2 % of the nominal fundamental value are analyzed, appropriate attenuation of interference distortions is crucial.

It was shown that dealing with different type of interference can by means of appropriate data acquisition system adjustment, shielding (i.e. coaxial cables, EMC-proof box), sensors adjustment and filtering. Of course sometimes it is difficult if even impossible to perfectly attenuate unwanted electromagnetic coupling. In that case appropriate interference assessment is needed which can be later taken into consideration during data processing and analysis.

7. Acknowledgment

The author would like to express his appreciation and gratefully acknowledge the contributions of Leif Svinth Christensen from Vestas Wind Systems A/S for his help in measurement sensors configuration.

The measurement campaign in AVV and GFS was sponsored by DONG Energy´s SIDER3.6 R&D project.

References

[1] Ł. H. Kocewiak, J. Hjerrild, and C. Leth Bak, "The Impact of Harmonics Calculation Methods on Power Quality Assessment in Wind Farms," in *International Conference on Harmonics and Quality of Power*, Bergamo, 2010, pp. 1-9.

[2] T. L. Clark, M. B. McCollum, D. H. Trout, and K. Javor, *Marshall Space Flight Center Electromagnetic Compatibility Design and Interference Control Handbook*. Alabama: National Aeronautics and Space Administration, 1995.

[3] R. P. Clayton, *Introduction to Electromagnetic Compatibility*, 2nd ed. New Jersey: John Wiley & Sons, 2006.

[4] C. M. Wiggins, D. E. Thomas, F. S. Nickel, T. M. Salas, and S. E. Wright, "Transient electromagnetic interference in substations," *IEEE Transactions on Power Delivery*, vol. 9, no. 4, pp. 1869-1884, Oct. 1994.

[5] D. E. Thomas, E. M. Wiggins, T. M. Salas, F. S. Nickle, and S. E. Wright, "Induced transients in substation cables: measurements and models," *IEEE Transactions on Power Delivery*, vol. 9, no. 4, pp. 1861-1868, Oct. 1994.

[6] M. Mohana Rao, M. Joy Thomas, and B. P. Singh, "Transients Induced on Control Cables and Secondary Circuit of Instrument Transformers in a GIS During Switching Operations," *IEEE Transactions on Power Delivery*, vol. 22, no. 3, pp. 1505-1513, Jul. 2007.

[7] L. H. A. de Medeiros, P. A. C. Rosas, Z. D. Lins, H. L. Ferreira, J. M. S. Melo, and N. G. Santos, "High frequency transients and electromagnetic interference within 69 kV substations," *Electric Power Systems Research*, vol. 81, no. 7, pp. 1534-1540, Jul. 2011.

[8] J. G. Webster, *The Measurement, Instrumentation and Sensors Handbook*. New York: Springer-Verlag, 2000.

[9] Department of Defense, *Global Positioning System Standard Positioning Service Signal Specification*, 4th ed. USA, September 2008.

[10] N. Kamarudin and Z. Mat Amin, "Multipath Error Detection Using Different GPS Receiver's Antenna," in *3rd FIG (International Federation of Surveyors) Regional Conference*, Jakarta, 2004, pp. 1-11.

[11] B. Ramakrishna Rao, A. D. Sarma, and Y. Ravi Kumar, "Technique to reduce multipath GPS signals," *Current Science*, vol. 90, no. 2, pp. 207-211, Jan. 2006.

[12] L. S. Christensen, M. J. Ulletved, P. Sørensen, T. Sørensen, T. Olsen, and H. K. Nielsen, "GPS Synchronized high voltage measuring system," in *Nordic Wind Power Conference*, Roskilde, 2007, pp. 1-6.

[13] R. Lai, Y. Maillet, F. Wang, S. Wang, R. Burgos, and D. Boroyevich, "An Integrated EMI Choke for Differential-Mode and Common-Mode Noise Suppression," *IEEE Transactions on Power Electronics*, vol. 25, no. 3, pp. 539-544, Mar. 2010.

[14] C. Gasquet and P. Witomski, *Fourier analysis and applications: filtering, numerical computation, wavelets*, 1st ed. New York: Springer-Verlag, 1999.

[15] J. R. Taylor, *An Introduction to Error Analysis: The Study of Uncertainties in Physical Measurements*, 2nd ed. University Science Books, 1997.

[16] S. W. Smith, *The Scientist and Engineer's Guide to Digital Signal Processing*, 2nd ed. San Diego, California: California Technical Publishing, 1999.

[17] Y. V. Prokhorov and V. Statulevičius, *Limit Theorems of Probability Theory*. Berlin: Springer, 2000.

[18] M. Grabe, *Measurement Uncertainties in Science and Technology*. Springer, 2005.

[19] R. M. Sheldon, *Introduction to Probability and Statistics for Engineers and Scientists*, 3rd ed. Elsevier Academic Press, 2004.

[20] C. E. Shannon, "Communication in the presence of noise," *Proceedings of the Institute of Radio Engineers*, vol. 37, no. 1, pp. 10-21, Jan. 1949.

[21] P. Billingsley, *Probability and Measure*, 3rd ed. John Wiley and Sons, 1995.

[22] L. M. Surhone, M. T. Timpledon, and S. F. Marseken, *Signal-to-noise Ratio: Signal (electronics), Noise (telecommunications), Bandwidth (signal processing), Amplitude, Decibel, Standard deviation, Signal to Noise Ratio (image processing)*. Betascript Publishing, 2010.

[23] M. Drosg, *Dealing with Uncertainties: A Guide to Error Analysis*, 2nd ed. Berlin: Springer-Verlag, 2009.

[24] C. Torrence and G. P. Compo, "A Practical Guide to Wavelet Analysis," *Bulletin of the American Meteorological Society*, vol. 79, pp. 61-78, 1998.

[25] I. Arana, "Switching overvoltages in offshore wind power grids. Measurements, modelling and validation in time and frequency domain," PhD Thesis, Technical University of Denmark, Copenhagen, 2011.